Feasibility and Effectiveness of Heat Pipe Cooling in End Milling Operations: Thermal, Structural Static, and Dynamic Analyses: A New Approach

Lin Zhu
School of Engineering,
Anhui Agricultural University,
Hefei 230036, P.R. China;

Mechanical Engineering Department,
University of Wisconsin,
Milwaukee, WI 53211

Tien-Chien Jen

Yi-Hsin Yen

Mechanical Engineering Department,
University of Wisconsin,
Milwaukee, WI 53211

Xiao-Ling Kong
School of Engineering,
Anhui Agricultural University,
Hefei 230036, P.R. China

In this paper, the feasibility and effectiveness of heat pipe cooling in end milling operations are investigated. A new embedded heat pipe technology was utilized to remove the heat generated at the tool-interface in end milling processes. Numerical studies involved four cases, including dry milling, fluid cooling, heat pipe cooling, and heat pipe cooling with cutting fluid supplied. The thermal, structural static, and dynamic characteristics of the end-mill were investigated using a numerical calculation with fast finite element plus solvers based on explicit finite element analysis software. The results demonstrate that the heat pipe end-mill is most feasible and effective in the actual end milling processes.
[DOI: 10.1115/1.4005037]

1 Introduction

The thermal aspect that occurs on the cutting tool during the material removal processes is a traditional concern. Thanks to the fact that the interaction among tool, chip, and work-piece usually causes not only tool wear but also chipping and thermal and mechanical cracking. For end milling, tool temperatures are particularly important because the tool used undergoes thermal shock in each revolution. The fast heating and cooling of the tool at work may result in considerable variations in cutting edge temperature. Furthermore, the heat generated during chip formation does not flow easily through the work-piece and chip, which increases the percentage of heat going to the tool, and makes the temperature variation even higher than before [1–3]. Consequently, this causes cracking perpendicular to the cutting edge. These increased cracks result either in chipping or, occasionally, in breakage of the cutting edge. To extend tool life, the most common approach is the use of cutting fluids flooding through the cutting zone. However, using cutting fluids often induce significantly negative impacts on environment, safety, operators' health and operating cost and especially the use of water-based cutting fluids in end milling operations usually increases temperature variation and, hence, thermal cracks [2,4,5].

Heat pipe cooling is considered to be an effective alternative to conventional methods for removing heat from a tool tip, allowing machining operations to be implemented in a dry and "green" fashion [6–12]. In this paper, the feasibility and effectiveness of heat pipe cooling in end milling operations are investigated. The thermal, structural static, and dynamic characteristics of the end-mill are predicted using a numerical calculation with fast finite element plus solvers based on explicit finite element analysis software.

2 FEA Model

2.1 Model Geometry. The model geometries of end-mills with and without heat pipe cooling were constructed by means of feature-based modeling method in SolidWorks before investigating their thermal, static, and dynamic characteristics. In terms of the real tool profile as shown in Fig. 1, the specifications of the end-mill are presented as follows (Fig. 2(*a*)):

- three-flute cutter, 20 mm ϕ_{head}, 18 mm ϕ_{end}, 125 mm long;
- rake angle $\gamma = 0°$, clearance angle $\alpha = 12°$, helix angle $\beta = 30°$;
- hard alloy material.

Based on Refs. [13–16], the dimensions of the heat pipe embedded in the solid cutter are 5.5 mm ϕ_{heatpipe}, 110 mm l_{heatpipe} (Fig. 2(*b*)).

2.2 FEA Modeling. The strategy in this study is based on high-density mesh, in which each solid element has 10 nodes for regions requiring high resolution. Four points Jacobian Check method for the distortion level of tetrahedral elements was utilized to mesh the entire end-mill and especially fine meshing at the tool tip. It is worth pointing out 8123 elements and 13,822 nodes were used for the solid end-mill, while 8812 elements and 14,307 nodes for the heat pipe end-mill.

3 Results and Discussion

3.1 Parameters and Computing Time. Only one of the three cutting edges needs to be numerically simulated in this study due to the end-mill being symmetrical and the cutting process being interrupted. Stainless steel was chosen for the work-piece material. Down-milling with passes in the longitudinal direction of the work-piece was used as a result of the fact that the thermal impact to the cutting tool during heating is larger in down milling than in up milling [3,5,15,16]. The associated parameters in the foregoing end milling process are presented as follows:

- Spindle speed $n = 5000r/\text{min}$, depth of cut $t = 5$ mm, width of cut $B = 20$ mm, feed per tooth $S_z = 0.1$ mm$/z$
  Based on Ref. [3,13,14], the loads acting on the cutting edge are presented below (Fig. 3)
- $F_t = 1377$ N, $F_a = 689$ N, $F_r = 565$ N

Fig. 1 Three-flute end mill

Contributed by the Manufacturing Engineering Division of ASME for publication in the Journal of Manufacturing Science and Engineering. Manuscript received December 9, 2010; final manuscript received September 5, 2011; published online October 14, 2011. Assoc. Editor: Tony Schmitz.

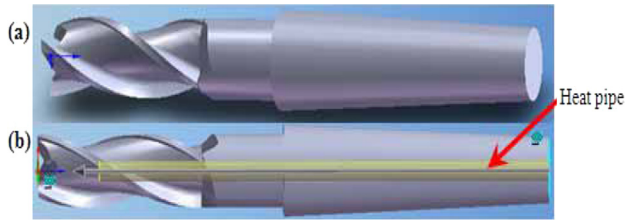

Fig. 2 Three-flute end-mill (*a*) without heat pipe and (*b*) with heat pipe

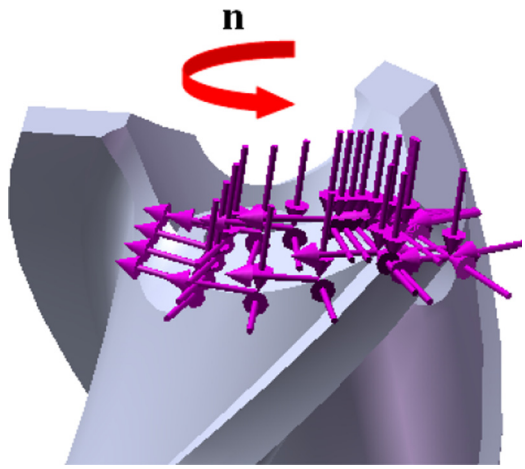

Fig. 3 The loaded end mill

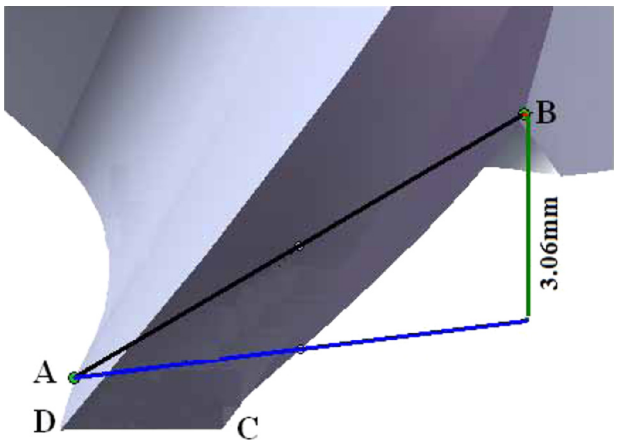

Fig. 4 Three-flute tool tip

The thermal and physical properties of the tool material are

- $E = 6 \times 10^{11}$ Pa, $\mu = 0.33$, $\rho = 14.7 \times 10^3$ kg/m^3, $\sigma_{bb} = 1470$ MPa
- $K = 35$ W/$(m \bullet k)$, $C_p = 50$ J/(kg $\bullet$ k), $\alpha = 5 \times 10^{-6}$/K

For end milling, an intermittent calculation was conducted in this study. H_{tooth} of the end mill is equal to 3.06 mm (Fig. 4), so T_{cutting} for one cutting edge was calculated as 0.0006 s in each tool revolution dependent on the geometric parameters of the standard three-flute end-mill and the prescribed operation conditions. This time actually represents the milling period from the cutting start point A to the cutting end point B, as illustrated in Fig. 4. A total calculation time of 0.0239 s elapsed for all simulations in this paper.

3.2 Temperature Distribution and Thermal Stress. The ambient temperature was set to be constant at 25 °C, and 100 °C

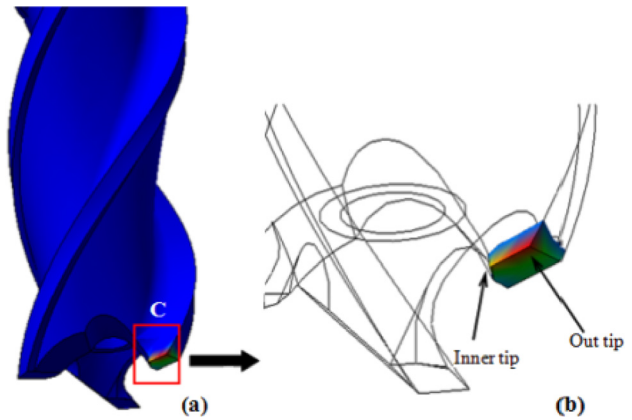

Fig. 5 (*a*) Temperature distribution on the tool tip and (*b*) detailed C of (*a*). Magnified view of the temperature distribution on the tool tip.

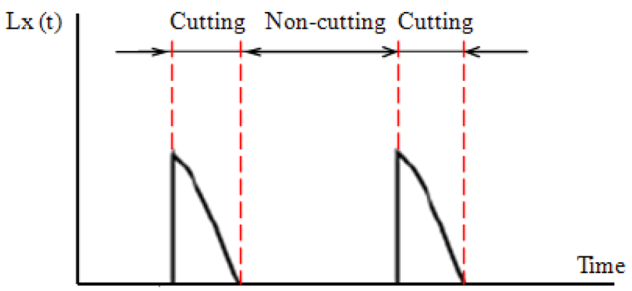

Fig. 6 Variation in tool-chip contact length in down milling

for the heat pipe under full operation condition with water as the working fluid. In view of the foregoing operation parameters, a calculated heat input of 8287 W was applied at the tip of the tool (Fig. 3), and with about 14.5% heat that enters the tool [3,14]. In addition, on all other surfaces imposed were the thermal boundary conditions seen above.

Seen from Fig. 5, for all the numerical simulation cases in this study, the peak temperatures occur at the end-mill tips, and the temperature at the outer tip is much higher than that at the inner tip.

The calculated results agree well with the actual milling operations. It is basically due to the facts as follows: new surface in end milling operations is generated as each tooth cuts away an arc-shaped segment. The undeformed chip thickness in the foregoing process is not constant but varies with tool rotation. The tool-chip constant length on the rake face varies with time (Fig. 6). According to Stephenson et al. [15,16], an end mill is modeled as a semi-infinite rectangular corner, $x \geq 0, y \geq 0, z \geq 0$, heated by a heat flux as shown in Fig. 7. Thus, the heat source dimension in the x-axis direction is a function of cutting time. For down milling processes, the depth of cut is the largest at the beginning of the cutting, and approximates 0 at the end, as shown in Fig. 8.

Figure 9 is a schematic illustration of the temperature variations at the outer tip with time. As observed, the maximum temperatures are approximate 1027 °C (1300 K) for dry milling, 767 °C (1040 K) for fluid cooling, 737 °C (1010 K) for heat pipe cooling, and 637 °C (910 K) for heat pipe cooling with coolant, respectively. Comparing Figs. 9(*b*) with 9(*c*), it could be inferred that the temperature using heat pipe does reduce faster than that using coolant (see the black arrows). This is because most of heat generated on the end-mill tip is quickly removed dependent on convection heat transfer by means of heat pipe. From the effect of the peak temperature viewpoint, the heat pipe cooling therefore outperforms the cases with dry milling, even with effective coolant, respectively.

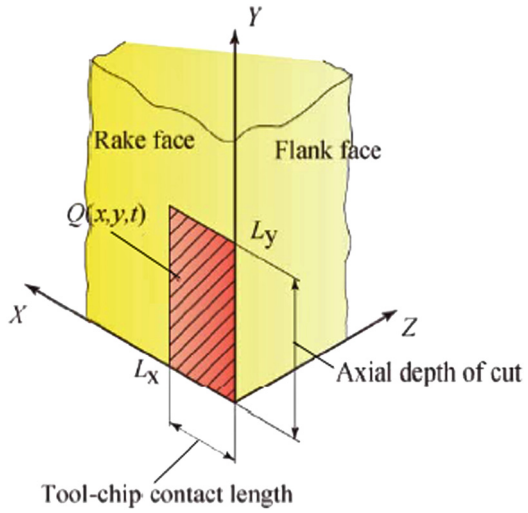

Fig. 7 Tool insert model

Figure 10 shows schematic for the variations of the thermal stress distributions at the end-mill tips under various cooling conditions. All of the maximum thermal stresses also occur at the tool tips within the same time as above and especially the thermal stress at the outer tip is larger than that at the inner tip. As observed, the thermal stresses at the outer tip are approximately 650 MPa, 500 MPa, 480 MPa, and 340 MPa for dry milling, fluid cooling, heat pipe cooling, and heat pipe cooling with coolant, respectively.

From Figs. 9 and 10, it can be seen that the peak temperature on the tool tip decreases from 1027 °C for the solid cutter to 737 °C for the heat pipe cooling by about 29% based on the same amount of heat input, and that the peak thermal stress also reduces from 650 MPa for dry milling to 480 MPa for the heat pipe cooling by an approximate factor of 1.4 under the same cooling conditions. Therefore, it can be concluded that with the aid of a heat pipe in the end milling operations, the probability of tool failure can be significantly reduced due to lower maximum temperature and thermal stress.

3.3 Structural Static and Dynamic Analysis. In end milling operations, the undeformed chip thickness varies with tool rotation, and tool-chip constant length on the rake faces also varies with time. Thus, the cutting edges must undergo much greater mechanical load due to their more numerous entrances and exits in the work-piece. This may generate cracks, chipping, and cutting edge breakage. Consequently, it is critical to choose a cutting tool with sufficient toughness and a rigid cutting edge in order to make the impacts less harmful to the tool. To verify the feasibility and effectiveness of the heat pipe end-mill, it is very essential to investigate its structural static and dynamic characteristics under the actual working conditions.

3.3.1 Static Stress and Strain Distributions. In view of the above-mentioned operation conditions, a clamp length, e.g., 9.29 mm was selected along the axis of the end mill (the red arrow in Fig. 11). The calculated results are presented in Figs. 11–13.

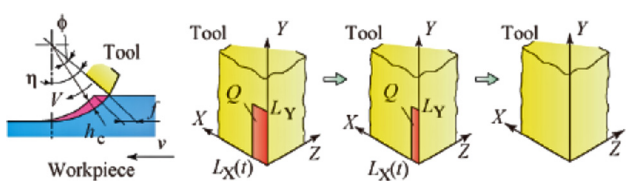

Fig. 8 Variation of heat source area in down milling

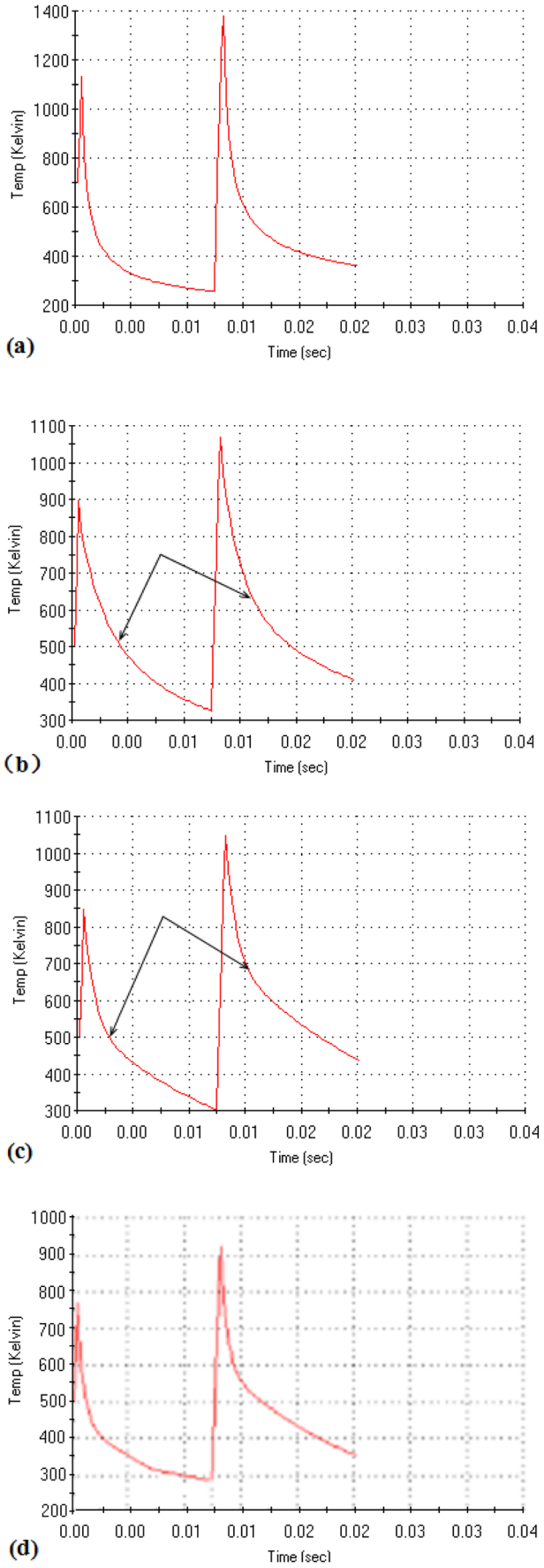

Fig. 9 Plots between the maximum temperatures on the tool tip vs. time (*a*) dry milling, (*b*) fluid cooling, (*c*) heat pipe cooling, and (*d*) heat pipe cooling with coolant

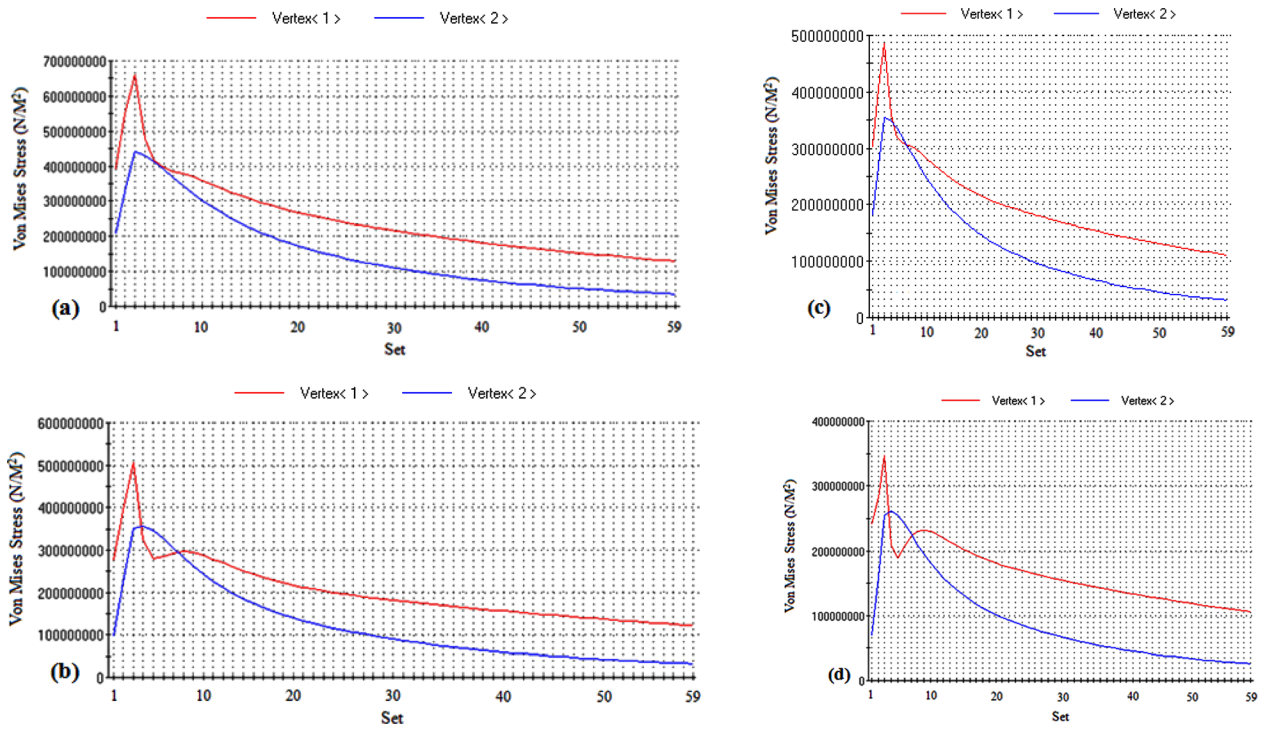

Fig. 10 The maximum thermal stresses in the cutting time (*a*) dry milling, (*b*) fluid cooling, (*c*) heat pipe cooling, and (*d*) heat pipe cooling with coolant

For end milling, the maximum static stresses, for the tool with or without heat pipe cooling, both occur at the tool tip (Figs. 11 and 12). The maximum static stresses for heat pipe tool and solid tool are 454.1 MPa and 409.4 MPa, respectively. With heat pipe embedded in the tool, a roughly 10% increase in static stress compared with the solid tool.

As illustrated in Fig. 13, the maximum strain for the solid tool only appears at the cutter tip (see the red ellipse), its value is 8.539×10^{-4}, while on the heat pipe cutter there exist two locations with the maximum strain, which is 8.555×10^{-4}. One also exists at the cutter tip, and the other appears at the clamp section (see the pink arrowhead).

As can be inferred from the above, the static stress and strain increase when the heat pipe end-mill is used. This is basically due to the fact that embedding a heat pipe in the solid tool decreases the inertia moment of the heat pipe tool and, therefore, increases the related bending deformation and bending stress. Note that for hard alloy material used for the end mill; however, its maximum bending strength is 1470 MPa, so the heat pipe tool in this study can satisfy the requirements of the milling operations. For the

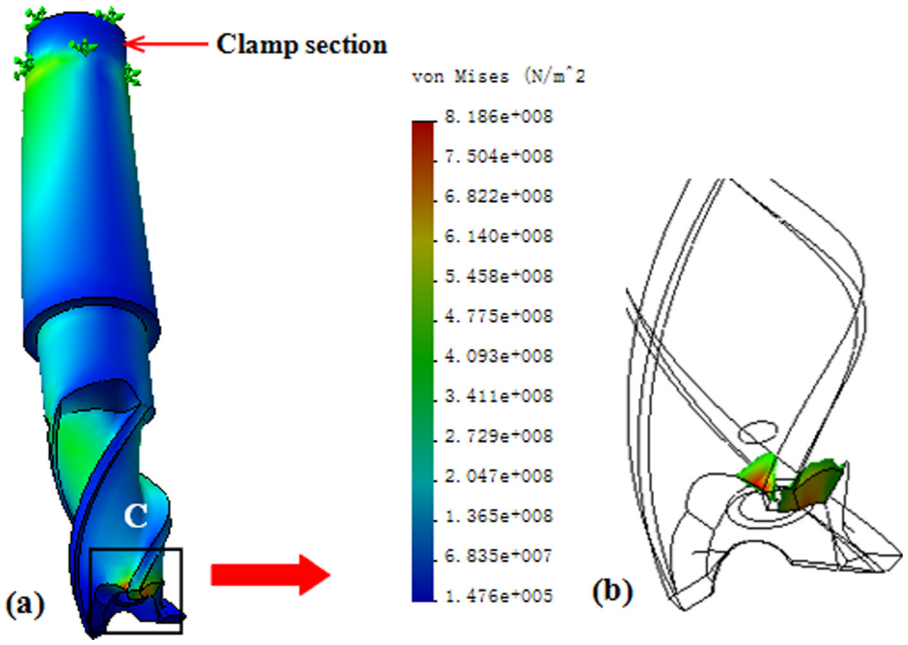

Fig. 11 (*a*) Static stress distribution on the solid end-mill and (*b*) detailed C of (*a*) Magnified view of the static stress on the tool

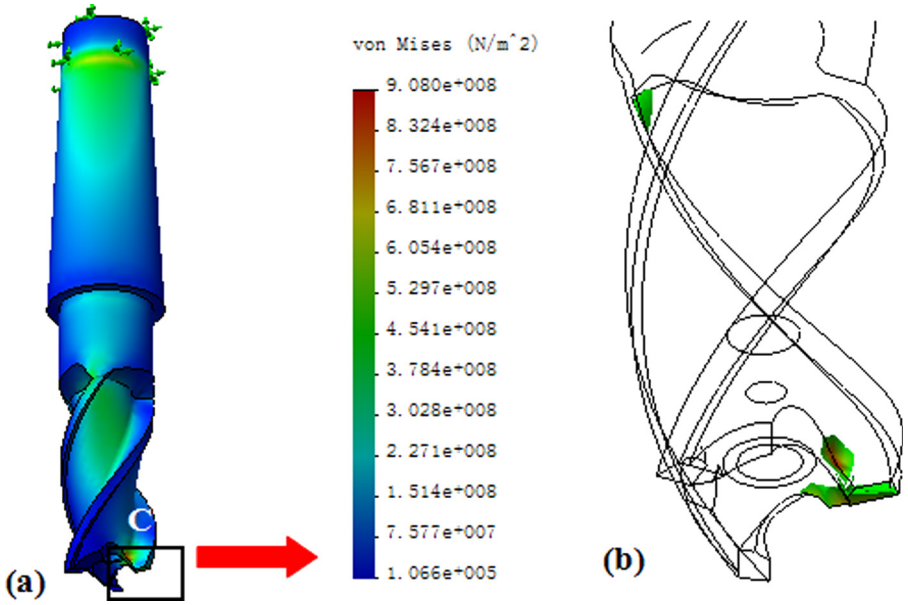

Fig. 12 (*a*) Static stress distribution on the heat pipe end-mill, (b) detailed C of (*a*) Magnified view of the static stress on the tool

higher static stress and strain in the heat pipe tool, the strength and stiffness of the main cutting zone, especially of the tool tip, could be improved by optimizing the geometric shape and configuration of the end-mill [3,14]. And also, it is found in the actual applications that optimizing the clamp length of the tool can lower the probability of the cutter resonating, especially of chattering and, consequently, decrease the bending deformation and bending stress [3,14]. This plays a critical role in extending the end-mill's lifetime.

3.3.2 Structural Dynamic Analysis. Mechanical impacts are also frequent in end milling operations due to the interrupted cutting inherent to it. The shocks and load variation on the tool gain importance and cause the chipping in the end of depth of cut area, which has deleterious effects on either the dimensional accuracies of the work-piece or the lifetime of the end milling operation system. Therefore, it is very essential to perform a structural dynamic analysis on the heat pipe end-mill.

In view of the actual vibrating state of the end-mill, 15 mode shapes are presented in this study dependent on the loads illustrated in Fig. 3. The frequencies of the solid end-mill are 1804.3 Hz (1), 1806.2 Hz (2), 7268.9 Hz (3), 7273.4 Hz (4), 10,325 Hz (5), 16,115 Hz (6), 16,910 Hz (7), 16,916 Hz(8), 20,616 Hz (9), 30,031 Hz (10), 30,049 Hz (11), 37,398 Hz (12), 41,311 Hz (13), 44,032 Hz (14), and 44,065 Hz (15), respectively.

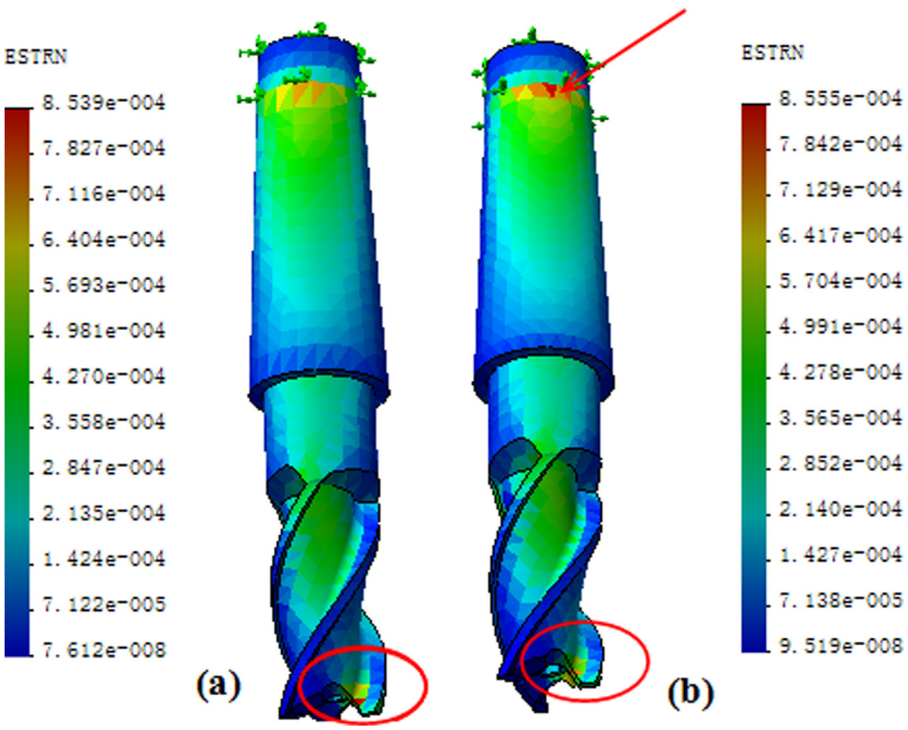

Fig. 13 Static strain distribution of the (*a*) solid end-mill and (*b*) heat pipe end-mill

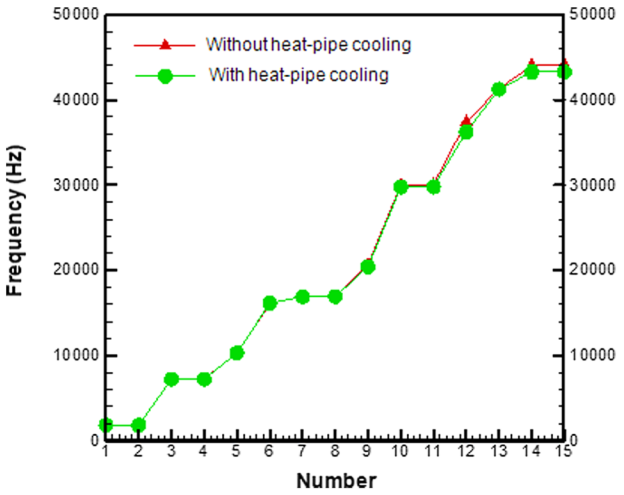

Fig. 14 Comparative vibration modes between a solid end-mill and a heat pipe end-mill under the clamp length 9.29 mm

Under the same machining conditions, the frequencies of the heat pipe end-mill are shown as follows: 1855.7 Hz (1), 1856.4 Hz (2), 7234.9 Hz (3), 7235.8 Hz (4), 10,319 Hz (5), 16,146 Hz (6), 16,894 Hz (7), 16,906 Hz (8), 20,413 Hz (9), 29,785 Hz (10), 29,791 Hz (11), 36,228 Hz (12), 41,241 Hz (13), 43,268 Hz (14), and 43,279 Hz (15), respectively.

Compared the vibration modes of the solid end-mill with those of the heat pipe end-mill, it could be seen from Fig. 14 that the vibration modes of the solid tool are a little higher than those of the heat pipe tool, which indicates that the solid end-mill deforms smaller than the heat pipe end-mill in the actual applications. This basically contributes to the fact that the higher frequency, for an end-mill in machining operations, leads to the larger rigidity. Significant vibration of the heat pipe tool may have deleterious effects on both the dimensional accuracy of a work-piece and the stability of the end milling operation system. All these could be improved by optimizing the milling speed. Furthermore, it is found in the industry applications that optimizing the clamp length of the end-mill does reduce the number of strong vibration modes in the end milling operations, thereby lowering the probability of the cutter resonating, especially of chattering [3,14].

4 Conclusion

From the thermal, structural static, and dynamic analyses point of view, the feasibility and effectiveness of the heat pipe end-mill were investigated. The numerical simulation results indicate that the peak temperature on the tool tip decreases from 1027 °C for the solid end-mill to 737 °C for the heat pipe end-mill by about 29% based on the same amount of heat input, and that the maximum thermal stress also reduces from 650 MPa for dry milling to 480 MPa for the heat pipe cooling by an approximate factor of 1.4 under the same cooling conditions. This implies that the use of a heat pipe in the end milling processes can effectively perform thermal management comparable to the flooding coolant cooling used pervasively in the machining industry.

The use of a heat pipe embedded the solid end-mill may increase the static stress and strain at the cutter tip and enhance the vibration frequency/magnitude due to its hollow center. However, for end milling, the foregoing negative effects could be improved by optimizing the geometric shape, configuration, and the clamp length of the heat pipe tool [3,14].

The numerical simulation evidences in this study, therefore, demonstrate that the use of heat pipe embedded in an end-mill is most feasible and effective and that the dry end milling can be achievable in the actual machining operations. Based on the results obtained in this work, several end mills with/without heat pipes have been manufactured and the results from testing are forthcoming in a future paper.

Acknowledgment

The authors would like to thank the financial support for the project from EPA-STAR Grant through RD833357.

Nomenclature

K = conductivity, $W/(m \bullet k)$
C_p = specific heat, $J/(kg \bullet k)$
ρ = density, kg/m^3
σ_{bb} = bending strength, MPa
G = shear modulus, Pa
μ = Poisson's ratio
E = elasticity modulus, Pa
α = coefficient of thermal expansion, K^{-1}
T = temperature, K
T_o = ambient temperature, K
T_{hp} = heat pipe surface temperature, K
q''_C = heat flux input in the cutting zone, W/m^2
k_T = thermal conductivity of the cutting tool material, $W/(m \bullet k)$

References

[1] Braghini, A., Jr., Diniz, A. E., and Filho, F. T., 2009, "Tool Wear and Tool Life in End Milling of 15-5 PH Stainless Steel Under Different Cooling and Lubrication Conditions," J. Adv. Manuf. Technol., **43**, pp. 756–764.
[2] Johnson, D., 1996, *Why Cutting Tools Fail. Tooling & Production*, Huebcore Communications Inc., Solon, Ohio.
[3] Trent, E., and Wright, P., 2000, *Metal Cutting*, Butterworth/Heinemann, Oxford, UK.
[4] Ding, Y., and Hong, S. Y., 1998, "Improvement of Chip Breaking in Machining Low Carbon Steel by Cryogenically Pre-Cooling the Workpiece," ASME J. Manuf. Sci. Eng., **120**, pp. 76–83.
[5] Palmai, Z., 1987, "Cutting Temperature in Intermittent Cutting," Int. J. Mach. Tool Manuf., **6**(2), pp. 261–274.
[6] Peterson, G. P., 1994, *An Introduction to Heat Pipes: Modeling, Testing, and Applications*, Wiley, New York.
[7] Judd, R. L., MacKenzie, H. S., and Elbestawi, M. A., 1995, "An Investigation of a Heat Pipe Cooling System for Use Turning on a Lathe," Int. J. Adv. Manuf. Technol., **10**(6), pp. 357–366.
[8] Ritcher, R., and Gottschlich, J. M., 1994, "Thermodynamics Aspects of Heat Pipe Operation," J. Thermodyn. Heat Transfer, **8**(2), pp. 334–340.
[9] Chan, S. H., Kanai, Z., and Yang, W. T., 1971, "Theory of a Rotating Heat Pipe," J. Nucl. Energy, **25**, pp. 479–487.
[10] Labataille, J., and Manjunathaiah, J., 1999, "Evaluation of Drilling With Heat Pipe Cooling," Lamb Technicon Machining Systems, Internal Report No. Lx-0437.
[11] Jen, T. C., Chen, Y. M., and Gutierrez, G., 2002, "Investigation of Heat Pipe Cooling in Drilling Applications. Part I: Preliminary Numerical Analysis and Verification," Int. J. Mach. Tools Manuf., **42**, pp. 643–652.
[12] Chiou, R. Y., Chen, J. S. J., Lin, L., and Cole, L., 2002, "Prediction of Heat Transfer Behavior of Carbide Inserts With Embedded Heat Pipes for Dry Machining," *Proceedings of ASME IMECE, Manufacturing Science and Engineering*, pp. 83–90.
[13] Toh, C. K., 2005, "Comparison of Chip Surface Temperature Between Up and Down Milling Orientations in High Speed Rough Milling of Hardened Steel," J. Mater. Process. Technol., **167**, pp. 110–118.
[14] Shaw, M. C., 2005, *Metal Cutting Principles*, Oxford University Press, New York.
[15] Jen, T. C., and Lavine, A. S., 1994, "Prediction of Tool Temperature in Interrupted Metal Cutting," *Proceedings of the 7th International Symposium on Transport Phenomena in Manufacturing Processes*, pp. 211–216.
[16] Stephenson, D. A., and Ali, A., 1992, "Tool Temperatures in Interrupted Metal Cutting," ASME J. Eng. Ind., **114**, pp. 127–136.